Design and Evaluation of Hierarchical Hybrid Automatic Modulation Classifier using Software Defined Radios

Jithin Jagannath, Dan O'Connor, Nicholas Polosky,
Brendan Sheaffer, Svetlana Foulke
ANDRO Advanced Applied Technology,
ANDRO Computational Solutions, LLC, Rome NY
{jjagannath, doconnor, npolosky,
bsheaffer, sfoulke}@androcs.com

Lakshmi N. Theagarajan, Pramod K. Varshney
Dept. of Electrical Engineering and Computer Science,
Syracuse University, Syracuse, NY
{ltheagar, varshney}@syr.edu

***Abstract*—Automatic modulation classification (AMC) is a key component of intelligent communication systems used in various military and cognitive radio applications. In AMC, it is desired to increase the number of different modulation formats that can be classified, reduce the computational complexity of classification, and improve the robustness and accuracy of the classifier. Generally, AMC techniques are classified into feature based (FB) and likelihood based (LB) classifiers. In this paper, we propose a novel hierarchical hybrid automatic modulation classifier (HH-AMC) that employs both feature based and likelihood based classifiers to improve performance and reduce complexity. As another major contribution of this paper, we implement and evaluate the performance of HH-AMC over-the-air (OTA) using software defined radios (SDRs) to demonstrate the feasibility of the proposed scheme in practice. Experimental evaluation shows high probability of correct classification (P_{cc}) for both linear and non-linear modulation formats including BPSK, QPSK, 8-PSK, 16-QAM, 32-QAM, CPFSK, GFSK and GMSK under lab conditions.**

I. Introduction and Background

Modern day communication systems backed by SDR technology aim to become more agile, secure and flexible in order to maximize the utilization of the available resources to accomplish various tasks and missions. In such communication systems, detecting and classifying the modulation format of the received signal becomes a necessary task for applications such as authentication, intruder detection, dynamic spectrum access and adaptive modulation. AMC has been studied for a number of years and a wide variety of techniques have been proposed in the literature. The AMC techniques are broadly classified into two types: feature based (FB) [1]–[7] and likelihood based (LB) methods [8]–[13]. The advantages of the FB approach include the ease of implementation, low computational complexity and a near-optimal performance when the signal power is sufficiently high. On the other hand, LB approach is optimal in the Bayesian sense, but it is known to be high in computational complexity.

Since each method has its own challenges and advantages, it is difficult to employ just one method to efficiently classify multiple modulation formats over different operational scenarios. To this end, we propose a hybrid approach that implements both FB and LB modulation classification schemes to efficiently classify multiple linear and non-linear modulation formats. Such a hybrid classification approach helps us to reduce both time and computational complexity.

Most of the previously known approaches in AMC have been evaluated via simulations under various assumptions. This is because their hardware implementation is extremely challenging and time consuming to test their performance in realistic scenarios [14]. But hardware based evaluation is critical to understand the practical challenges so that the AMC algorithms can be refined to ensure successful transition to commercial and military communication systems. SDRs provide a flexible platform that can expedite rapid development and experimentation [15]. There are very few reported works that discuss the performance evaluation of AMC using actual hardware [16]–[19]. In this paper, we design an AMC technique to efficiently classify multiple modulation formats and evaluate its performance in practice using SDR.

The major contributions in this paper can be summarized as follows,

- We propose a decision tree based novel hierarchical hybrid AMC to classify both linear and non-linear modulation formats.
- To improve the efficiency of HH-AMC, we empirically identify the appropriate AMC technique to be employed at each node of the decision tree in HH-AMC using parameters such as the time taken to reach a decision (T_{dec}) and the probability of correct classification (P_{cc}).
- We study the practical feasibility of the proposed scheme using a hardware implementation in SDR and show that

[1]ACKNOWLEDGMENT OF SUPPORT AND DISCLAIMER:(a) Contractor acknowledges Government's support in the publication of this paper. This material is based upon work supported by the US Air Force Research Laboratory under AFRL Contract No. FA8750-16-C-0085. (b) Any opinions, findings and conclusions or recommendation expressed in this material are those of the author(s) and do not necessarily reflect the views of AFRL.

978-1-5090-4228-9/17/$31.00 ©2017 IEEE

it achieves very good performance.

The rest of the paper is organized as follows. In Sections II and III we discuss the performance and computational complexity of the LB and FB classifiers, respectively. Using the performance-complexity trade-off study from Sections II and III, we propose a hierarchical hybrid classifier in Section IV. The results of the hardware experiments on the proposed HH-AMC are also presented in Section IV. Finally, the conclusions are presented in Section V.

II. Likelihood based classifier

In this section, we investigate the performance and computational complexity of the LB classifiers for AMC. This investigation helps us to identify under what conditions it is advantageous to use LB classifiers over the other techniques.

An LB classifier computes the likelihood of the received signal for each modulation format in the dictionary. Direct computation of the maximum likelihood value is computationally very complex. It was reported in [11] and [13] that the computational complexity of the LB approach can be reduced using the expectation-maximization (EM) algorithm. Overall, the performance of the LB schemes is known to be optimal in the Bayesian sense but the LB methods are computationally intensive. Therefore, it is important to reduce the time taken to reach a decision (T_{dec}) for the LB methods to ensure that the decision is available within the application's time requirements.

A. *Overview of expectation-maximization (EM) algorithm*

Consider a receiver that is observing a linearly modulated signal that undergoes block fading. The down-converted RF signal at the receiver can be expressed as,

$$y(t) = ae^{j\theta}\sum_{n} I_l g(t-nT) + w(t), \qquad 0 \le t \le T_0 \tag{1}$$

where $a > 0$ is the channel gain, $\theta \in [-\pi, \pi)$ represents the channel phase, I_l is the l^{th} complex constellation of the transmitted symbol, $g(t)$ is the transmit pulse, T_o is the observation interval, T is the symbol duration, $w(t)$ is the additive complex zero-mean white Gaussian noise process at the receiver with two-sided power spectral density (PSD) $N_0/2$. In this model, $\{I_l, a, \theta, N_0\}$ are the unknown signal parameters. Among these, $u \triangleq [a, \theta, N_0]$ is the deterministic unknown parameter vector. Let S be the number of candidate modulation formats under consideration, and let $I_l^{(i)}$ denote the l^{th} constellation symbol corresponding to the i^{th} modulation format where $i \in \{1, ..., S\}$. The sampled baseband signal at the receiver is given by

$$y(mT_s) = ae^{j\theta}\sum_{n} I_l g(mT_s - nT) + w(mT_s), \quad 0 \le mT_s \le T_0 \tag{2}$$

where T_s is the sampling time such that $T = cT_s$ for some positive integer c, and m is a non-negative integer.

The goal is to identify the correct modulation format from S candidate formats (or equivalently the corresponding hypothesis) based on y. Let $\Lambda_i(u)$ represent the log-likelihood (LL) function of the i^{th} modulation format. The method of moments (MoM) is used to initialize the values of the unknown parameters before the estimation process. A detailed description of the EM algorithm can be found in [11]. For immediate reference, the steps in EM algorithm are listed in Algorithm 1.

Algorithm 1 EM based AMC

1: Initiate S parallel threads
2: At each thread i corresponding to each modulation
3: Set stopping parameter ε
4: iter=0
5: Set r=0. Initialize ${\hat{u}_i}^{(0)}$ using MoM
6: Compute $\Lambda_i({\hat{u}_i}^{0})$
7: Set $r = r + 1$
8: Compute $\hat{a}^{r+1}$
9: Compute $\hat{\theta}^{r+1}$
10: Compute ${\hat{N}_0}^{r+1}$
11: Compute $\hat{\Lambda}_i(u_i^{(r+1)})$
12: **if** $\Lambda_i({\hat{u}_i}^{(r+1)}) - \Lambda_i({\hat{u}_i}^{r}) > \Lambda_i({\hat{u}_i}^{r}) * \varepsilon$ **then**
13: go to Step 7
14: **else**
15: $\hat{u}_i = {\hat{u}_i}^{(r+1)}$ and continue
16: **end if**
17: Final decision $\hat{i} = argmax_i \Lambda_i(\hat{u}_i)$

Before we discuss the performance of the EM algorithm, we briefly describe the hardware testbed in which all the experiments were performed.

B. *Testbed configuration*

The testbed consists of two USRP (universal software radio peripheral) X300s that are used as transmitter and receiver as shown in Fig. 1. They are equipped with CBX-120 daughterboards, which cover frequency ranges from 1.2 GHz to 6 GHz with up to 120 MHz of instantaneous analog bandwidth. The analog-to-digital and digital-to-analog converters on the motherboard use a 200 MHz master clock and sample at 200 MS/s and 800 MS/s, respectively. The Linux-based host PC interfaces with the USRP using a Gigabit Ethernet (GigE) connection.

The SDR setup used to perform classification is similar to [15], but the capabilities have been significantly enhanced by adding multiple classification techniques to classify a wider range of modulation formats at lower computational complexity. Additionally, the algorithms and pre-processor blocks are implemented in C++, rather than Python, to improve the computational efficiency. The received samples are processed by an energy detector to separate actual signal transmissions from noise. Next, the samples go through an automatic gain control (AGC) block before being sent to the selected classifier blocks. The transmitter is set to transmit at a center frequency of 2.41 GHz. The transmitter's sampling rate is set to 1 MS/s, whereas the receiver's sampling rate is set at 5 MS/s. This is on the basis of the assumption that when the receiver is unaware of the transmitter's sampling rate, it will operate at

Fig. 1: Software defined radio testbed

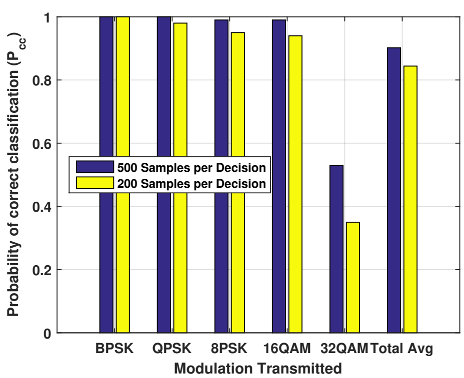

Fig. 2: P_{cc} vs Number of samples

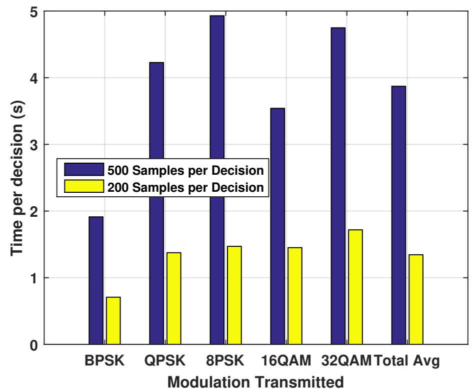

Fig. 3: T_{dec} vs Number of samples

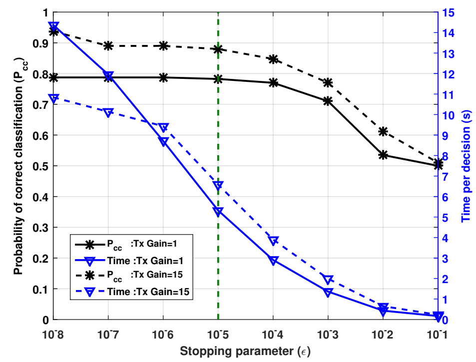

Fig. 4: *Pcc* & T_{dec} vs Stopping parameter (with 32QAM)

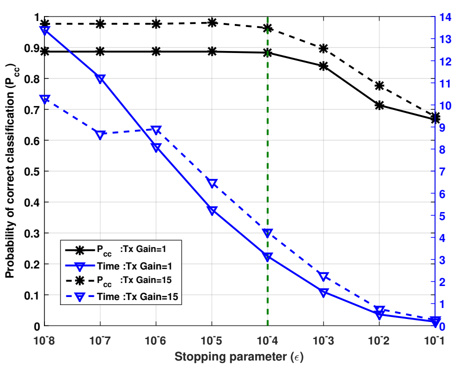

Fig. 5: *Pcc* & T_{dec} vs Stopping parameter (without 32QAM)

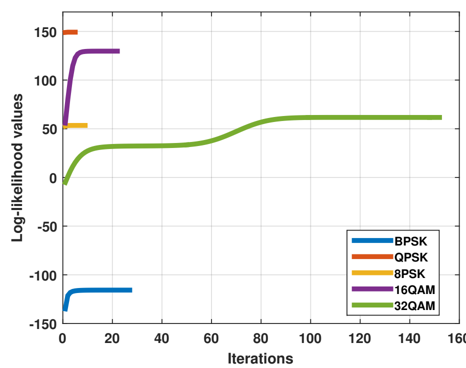

Fig. 6: Log-likelihood values vs Iterations

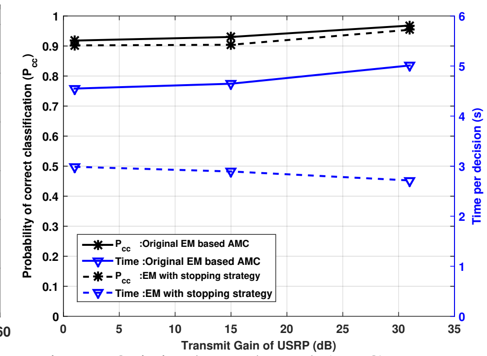

Fig. 7: Original EM based AMC vs EM with the proposed stopping strategies.

the highest possible sampling rate to oversample the received signal. This testbed emulates a realistic flat fading channel in the lab. All the results obtained with the testbed are averaged over several instances.

We analyze the performance of the LB algorithm in three different experimental scenarios. The parameters pertaining to each experimental scenario are depicted in Table I. Each scenario evaluates the performance of the AMC algorithm for different system parameters using the USRPs in the laboratory setup.

C. Parameters jointly influencing T_{dec} and P_{cc}

As mentioned earlier, one major shortcoming of the LB classifier is the computational complexity. Even though the EM algorithm reduces the complexity of computing the likelihoods, the iterative nature of the EM algorithm results in a large value of T_{dec}. So, it is essential to study the trade-off between P_{cc} and T_{dec}. We conducted the following experiments to understand this trade-off and improve the AMC algorithm accordingly.

Experiment 1: Here, we determine how P_{cc} and T_{dec} vary as the number of samples (N_s) used per decision is changed.

TABLE I: Parameter values used in experiments

Parameters	Experiment 1	Experiment 2	Experiment 3
Number of samples	500 & 200	500	500
Transmit Gain	15 dB	1 dB & 15 dB	1 dB, 15 dB & 31 dB
Receiver Gain	15 dB	15 dB	15 dB
Stopping parameter(ε)	10^{-6}	10^{-8} to 10^{-1}	10^{-5}
Number of decisions	100	100	100

Figures 2 and 3 depict the change in P_{cc} and T_{dec}, respectively, when N_s is reduced from 500 to 200 in Exp.1. The decrease in P_{cc} of the classifier is relatively small when BPSK, QPSK, 8PSK and 16QAM are transmitted; whereas, T_{dec} decreases by at least 50% for each modulation. This shows that choosing a smaller N_s can improve T_{dec} considerably without drastically deteriorating the overall performance of the classifier if the dictionary of modulation formats is known *a priori* to contain lower order modulations formats.

Experiment 2: Another important parameter that influences P_{cc} and T_{dec} significantly is the value of the stopping parameter ε used in the EM algorithm. Fig. 4 (modulation dictionary: { BPSK, QPSK, 8PSK and 16QAM}) and Fig. 5 (modulation dictionary: { BPSK, QPSK, 8PSK, 16QAM and 32QAM}) depict the effect on P_{cc} and T_{dec} simultaneously as ε changes. In Figures 4 and 5, the Y-axis on the right hand-side represents P_{cc} and the left hand side represents T_{dec}. As expected, both P_{cc} and T_{dec} decrease as ε increases. However, P_{cc} and T_{dec} decrease at different rates as ε increases. It can be observed from Figures 4 and 5 that by reducing the value of ε beyond a certain value, the performance gain achieved in terms of P_{cc} is relatively small. On the other hand, T_{dec} continues to increase at a considerable rate as ε decreases. Therefore, it is important to determine an efficient operating point. Such a point corresponds to the least time taken by the EM algorithm to make a decision without a significant loss in performance. In both Figures 4 and 5, we evaluated the performance for two transmit gains 1 dB and 15 dB corresponding to two SNR conditions ($\sim 20-25$ dB and $\sim 30-35$ dB respectively). From this experiment, it is observed that the value of ε to be chosen as the operating point depends more on the modulation formats in the dictionary rather than the SNR of the signal itself. Accordingly, it is deduced that the operating value of ε for the dictionaries in Figures 4 and 5 can be 10^{-5} and 10^{-4}, respectively, regardless of the transmit gain.

Experiment 3: Here, we empirically study the number of iterations required by the EM algorithm to converge to the final likelihood value for each modulation format. Due to the nature of the computations in the EM algorithm [9], [11], the LL values for each modulation format can be calculated in parallel. Figure 6 gives the LL values calculated using the EM algorithm in parallel threads for each modulation format against the number of EM iterations. Each of these threads are terminated when their is no significant change in the LL values. In this example, the LL computation corresponding to 32QAM takes much longer computation time, even though it does not converge to the highest value compared to the LL values of the other modulation formats. This motivates us to investigate an efficient stopping criterion for the EM algorithm to reduce T_{dec} without affecting P_{cc}.

Accordingly, from our experimental observations, we propose the following exit strategies for the EM algorithm to reduce the overall execution time. This exit strategy is listed below.

- **Step 1**: If the current LL value for BPSK is at least λ_1 times greater than the remaining modulation threads, then terminate all computations and classify the signal as BPSK.
- **Step 2**: If the condition in Step 1 is not satisfied, then check if the LL value of QPSK is at least λ_2 times greater than that of 8PSK, and the LL value of 16QAM is λ_3 times greater than that of 32QAM. If this condition is satisfied, then stop the LL computations for 8PSK and 32QAM.
- **Step 3**: Track the LL values of the last running thread and terminate the thread if it has the highest value. Otherwise, terminate the thread if it is less than λ_4 times the largest LL value among all the other threads ($\lambda_4 \in (0,1)$).

In this strategy, Step 2 eliminates the unlikely modulation formats early by exiting the iteration loop. Step 3 terminates the only thread that is running if the corresponding LL value is already the highest or if it is small enough to indicate a very low chance of being the relevant modulation.

In Fig. 7, we compare the values of P_{cc} and T_{dec} of the EM algorithm with and without the stopping strategies for different transmit gains. As we can observe from Fig. 7, the EM based AMC with the proposed stopping strategy reduces T_{dec} by up to 45% without a significant drop in the value of P_{cc}. From several lab experiments we find that these stopping strategies perform well. The values of the parameters $\lambda_1, \cdots, \lambda_4$ computed empirically are listed in Table V

III. Feature based classifiers

FB approaches use features that are extracted from the instantaneous amplitude, phase and frequency of the received signal to make a classification decision. Some FB approaches use signal statistics based algorithms which utilize cumulants and their cyclic variants [3], [4]. In this section, we discuss several FB classifiers, their advantages, and performance-complexity trade-off. Though it is theoretically known that the values of the features discussed below are different for different modulation formats, we study their practical range of values and the feasibility of using them in a practical AMC hardware.

A. Variance of instantaneous amplitude

The variance of the received signal amplitude is given by,

$$\sigma^2_{amp} = \frac{\sum_{N_s}(|y(t)| - \mu)^2}{N_s}, \quad (3)$$

where $|y(t)|$ is the absolute value of the over-sampled signal and μ represents the mean of N_s samples. The average value of σ^2_{amp} for different modulation formats is presented in Fig. 8 for different values of N_s (64, 128, 256 and 512). The signal was oversampled by five times and both the transmit and receive gains were set to 15 dB. It can be observed that this feature clearly distinguishes FSK signals (CPFSK, GFSK, GMSK) from the rest of the modulation formats (PSKs and QAMs). The reason for higher values observed for QAM are due to the variation in the amplitude of the signal; whereas, oversampling captures the transitions between different symbols of PSK, leading to an amplitude variation. Therefore, we identify σ^2_{amp} as the low-complexity feature to differentiate FSK signals from PSK and QAM signals.

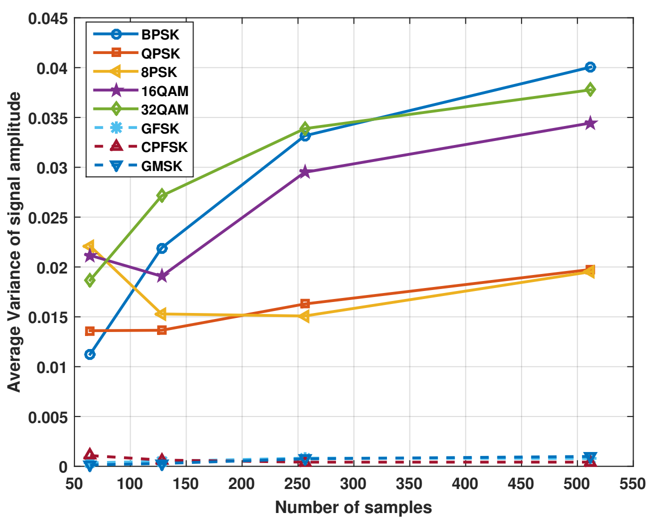

Fig. 8: Variance of amplitude for different modulation formats.

B. Maximum value of PSD of the normalized-centered instantaneous amplitude

Now, we consider the maximum value of PSD of the normalized-centered instantaneous amplitude [1] given as

$$\gamma_{max} = \frac{max|FFT(a_{cn}(n))|^2}{N_s}, \quad (4)$$

where $a_{cn}(n) \triangleq \frac{a(n)}{m_a} - 1$, $m_a = \frac{1}{N_s}\sum_{n=1}^{N_s} a(n)$, and $a(n)$ is the absolute value of the complex-valued received signal. The normalization by the instantaneous amplitude is required to compensate for the channel gain. The feature γ_{max} gives us a measure of deviation of the PSD of the signal from its average value. Traditionally, γ_{max} has been used to differentiate PSK signals from FSK signals [1]. In contrast, we use the average value of γ_{max} to classify CPFSK, GFSK and GMSK. The minimum, mean and maximum values of γ_{max} computed experimentally are provided in Table II. It has been observed that the values of γ_{max} for these signals do not overlap even at different transmit gains. However, further investigation is required to study their performance at very low values of SNR.

TABLE II: γ_{max} values of CPFSK, GFSK, GMSK

Modulation	CPFSK		GFSK		GMSK	
Tx gain	1dB	15dB	1dB	15dB	1dB	15dB
Minimum	0.36	0.43	6.00	5.83	11.26	11.5
Mean	0.24	0.30	4.43	4.46	8.49	8.55
Maximum	0.13	0.20	3.41	3.31	6.78	6.36

C. Higher order statistics

Features based on higher order statistics are quite useful in classifying amplitude and phase modulated signals at lower computational complexity compared to LB algorithms. Cumulants are one such higher order statistics that can be used to classify these modulation formats efficiently [4], [5]. Cumulants are statistical measures that are known to be invariant to certain distortions in random signals. Hence, they are very suitable for the purpose of modulation classification. The cumulant of a random signal is a function of two parameters,

- n: the order of the cumulant
- k: the number of conjugations involved in the computation of the cumulant ($k \leq n$).

The nth order cumulant of the random signal y with k conjugations can be computed as

$$C_{nk} = \sum_{p}^{\text{No. of partitions in } n} (-1)^{p-1}(p-1)! \prod_{j=1}^{p} \mathbb{E}\{y^{n_j - k_j} y^{*k_j}\}, \quad (5)$$

where n_j and k_j correspond to the subsets in the partition j. In our experiments, we use the fourth order cumulants to distinguish between PSK and QAM signals. Specifically, we use C_{42} and C_{40} for classification. These cumulants can be evaluated as

$$C_{42} = \mathbb{E}(|y|^4) - |\mathbb{E}(y^2)|^2 - 2\mathbb{E}(|y|^2)^2, \quad (6)$$

$$C_{40} = \mathbb{E}(y^4) - 3\mathbb{E}(y^2)^2. \quad (7)$$

We use the ratio C_{40}/C_{42} for the purpose of modulation classification. The ratio avoids the need for any normalization required due to different signal energies or channel gains.

We evaluate the average value of C_{40}/C_{42} computed using 2048 received signal samples. The minimum, maximum and mean values observed for PSK and QAM signals are listed in Table III at two different transmit gains. The values do not overlap even while using different transmit gains. This indicates that a reliable threshold can be set to differentiate PSKs from QAMs using this feature.

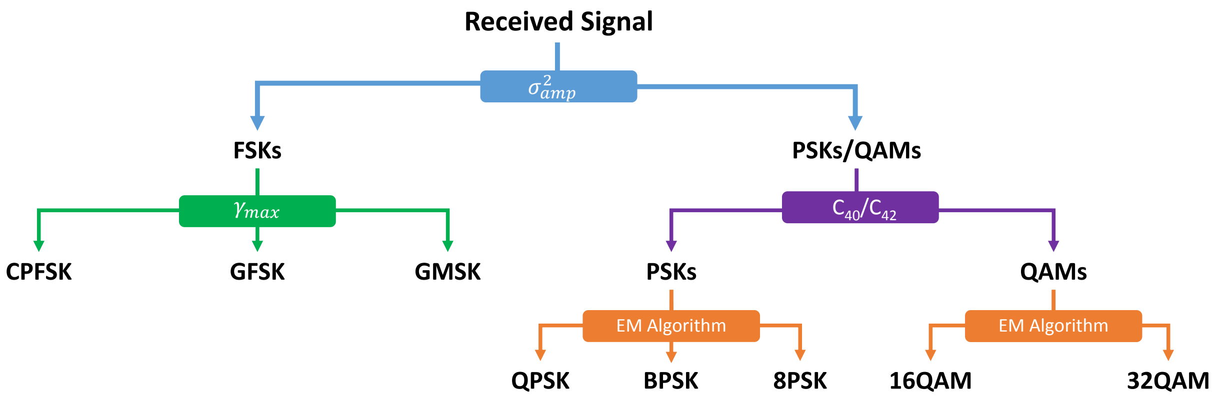

Fig. 9: Decision tree of the proposed HH-AMC.

TABLE III: Ratio of C_{40}/C_{42} of PSKs and QAMs

Modulation	PSKs		QAMs	
Tx gain	1dB	15dB	1dB	15dB
Minimum	0.83	0.92	1.27	1.29
Mean	1.05	1.08	1.37	1.37
Maximum	1.36	1.18	1.47	1.45

IV. Hierarchical Hybrid Automatic Modulation Classifier (HH-AMC)

In this section, we discuss how the AMC techniques implemented and evaluated thus far are used to form a novel HH-AMC. The decision tree of the proposed HH-AMC is depicted in Fig. 9. The dictionary of the modulation formats that we consider include CPFSK, GFSK, GMSK, BPSK, QPSK, 8PSK, 16QAM and 32QAM.

Using the observations made from the experiments conducted thus far, we identified which AMC technique (of those discussed in Sections II and III) could be used at each node of the decision tree to improve the overall performance and efficiency of the AMC system. The first level of the classifier uses the value of σ^2_{amp} to distinguish FSK signals from PSK and QAM signals. This is because, the IQ samples of FSK signals stay on the unit circle, and so, the value of σ^2_{amp} is extremely low for FSK signals compared to the rest. The second level of the hierarchical classifier uses two FB classifiers. The value of γ_{max} is used to classify the FSK signals as CPFSK, GFSK or GMSK. On the other hand, the fourth order cumulants are used to differentiate between PSK and QAM signals. At the final stage of classification, the computationally intensive EM based ML classifier is used to identify the modulation order in PSK or QAM signals.

To evaluate the performance of the proposed HH-AMC, we conducted an experiment using the parameters shown in Table V. The received signal is oversampled by five times. The number of samples used per decision for computing σ^2_{amp}, cumulants, γ_{max}, and for the EM based ML algorithm are 512, 2048, 50×512 and 512 respectively. The decisions are recorded in the form of a confusion matrix shown in Table IV. An ideal confusion matrix would have ones along its diagonal and zeros elsewhere. This would indicate that all the classification decisions were correct.

TABLE V

Parameters	Values
Transmit gain	1 dB
Receiver gain	15 dB
λ_1	2
λ_2 and λ_3	1.5
λ_4	0.5
No. of decisions	100

With the exception of 32QAM, the classification accuracy P_{cc} is 0.99 or greater. The only modulation format with relatively higher number of misclassifications is 32QAM. We noticed that when the transmit gain is increased to 31 dB, while keeping every other parameter the same, the value of P_{cc} for 32QAM increased from 0.57 to 0.81. Further, When the sampling rate at the receiver was reduced to 2 MS/s, the value of P_{cc} of 32 QAM increased to 0.93. This shows that high SNR and appropriate sampling rate improve the classification performance. More importantly, the T_{dec} for the overall classification was reduced significantly.

V. Conclusions

In this paper, we have proposed a novel HH-AMC that combines both FB and LB classifiers to efficiently classify signals of the following modulation formats: BPSK, QPSK, 8-PSK, 16-QAM, 32-QAM, CPFSK, GFSK, and GMSK. To establish its feasibility and practicality, we performed OTA evaluation on the USRP based testbed. The experiments showed high values (> 0.99) of P_{cc} for all modulation formats except 32QAM. Additionally, a significant improvement was achieved in the average T_{dec} of the classifier. In the future, we will investigate the performance of HH-AMC at lower SNRs and challenging channel conditions to establish the practical operational range. We will also investigate efficient

TABLE IV: Confusion matrix of the proposed HH-AMC

		HH-AMC Decision Probability								T_{dec} (ms)
		CPFSK	**GFSK**	**GMSK**	**BPSK**	**QPSK**	**8PSK**	**16QAM**	**32QAM**	
Tx Modulation	**CPFSK**	**1**	-	-	-	-	-	-	-	**145.56**
	GFSK	-	**1**	-	-	-	-	-	-	**156.31**
	GMSK	-	-	**1**	-	-	-	-	-	**138.79**
	BPSK	-	-	-	**1**	-	-	-	-	**144.21**
	QPSK	-	-	-	-	**0.99**	**0.01**	-	-	**184.30**
	8PSK	-	-	-	-	**0.01**	**0.99**	-	-	**242.26**
	16QAM	-	-	-	-	-	-	**0.99**	**0.01**	**1916.38**
	32QAM	-	-	-	-	-	-	**0.43**	**0.57**	**5769.40**

low-complexity methods to improve the performance of the AMC algorithm for higher order QAM and other modulation formats.

References

[1] A. Hazza, M. Shoaib, S. AlShebeili, and A. Fahd, "Automatic modulation classification of digital modulations in presence of HF noise." *EURASIP Journal on Adv. in Signal Processing*, vol. 2012, p. 238, 2012.

[2] A. Kubankova, J. Prinosil, and D. Kubanek, "Recognition of Digital Modulations Based on Mathematical Classifier," in *Proc. of the European Conference of Systems (ECCS)*, Stevens Point, WI, 2010.

[3] O. Dobre, A. Abdi, Y. Bar-Ness, and W. Su, "Selection combining for modulation recognition in fading channels," in *Proc. of IEEE Military Communications Conference (MILCOM)*, Oct 2005.

[4] A. Swami and B. M. Sadler, "Hierarchical digital modulation classification using cumulants," *IEEE Transactions on Communications*, vol. 48, no. 3, pp. 416–429, Mar 2000.

[5] D. C. Chang and P. K. Shih, "Cumulants-based modulation classification technique in multipath fading channels," *IET Communications*, vol. 9, no. 6, pp. 828–835, 2015.

[6] L. Han, F. Gao, Z. Li, and O. Dobre, "Low Complexity Automatic Modulation Classification Based on Order-Statistics," *IEEE Transactions on Wireless Communications*, vol. PP, no. 99, pp. 1–1, 2016.

[7] T. Cai, C. Wang, G. Cui, and W. Wang, "Constellation-wavelet transform automatic modulation identifier for M-ary QAM signals," in *Proc. of IEEE 26th Annual International Symposium on Personal, Indoor, and Mobile Radio Communications (PIMRC)*, Valencia, Spain, Aug 2015, pp. 212–216.

[8] F. Hameed, O. Dobre, and D. Popescu, "On the likelihood-based approach to modulation classification," *IEEE Transactions on Wireless Communications*, vol. 8, no. 12, pp. 5884–5892, December 2009.

[9] T. Wimalajeewa, J. Jagannath, P. K. Varshney, A. Drozd, and W. Su, "Distributed asynchronous modulation classification based on hybrid maximum likelihood approach," in *Proc. of IEEE Military Communications Conference (MILCOM)*, Tampa, FL, Oct 2015.

[10] Y. Zhang, N. Ansari, and W. Su, "Optimal Decision Fusion Based Automatic Modulation Classification by Using Wireless Sensor Networks in Multipath Fading Channel," in *Proc. of IEEE Global Telecommunications Conference (GLOBECOM)*, Houston, TX, Dec 2011.

[11] O. Ozdemir, R. Li, and P. Varshney, "Hybrid Maximum Likelihood Modulation Classification Using Multiple Radios," *IEEE Communications Letters*, vol. 17, no. 10, pp. 1889–1892, October 2013.

[12] B. Dulek, O. Ozdemir, P. K. Varshney, and W. Su, "Distributed Maximum Likelihood Classification of Linear Modulations over Nonidentical Flat Block-Fading Gaussian Channels," *IEEE Transactions on Wireless Communications*, vol. 14, no. 2, pp. 724–737, February 2015.

[13] O. Ozdemir, T. Wimalajeewa, B. Dulek, P. K. Varshney, and W. Su, "Asynchronous Linear Modulation Classification with Multiple Sensors via Generalized EM Algorithm," *IEEE Transactions on Wireless Communications*, vol. 14, no. 11, pp. 6389–6400, November 2015.

[14] S. Foulke, J. Jagannath, A. Drozd, T. Wimalajeewa, P. Varshney, and W. Su, "Multisensor Modulation Classification (MMC): Implementation Considerations – USRP Case Study," in *Proc. of IEEE Military Communications Conference (MILCOM)*, Oct 2014.

[15] J. Jagannath, H. M. Saarinen, and A. L. Drozd, "Framework for automatic signal classification techniques (FACT) for software defined radios," in *Proc. of IEEE Symposium on Computational Intelligence for Security and Defense Applications (CISDA)*, Verona, NY, May 2015.

[16] T. J. O'Shea, T. C. Clancy, and H. J. Ebeid, "Practical signal detection and classification in GNU Radio," in *Proc. of SDR Forum Technical Conference*, 2007.

[17] H. Hosseinzadeh, "Tracking performance of large margin classifier in automatic modulation classification with a software radio environment," *Journal of Systems Engineering and Electronics*, vol. 25, no. 5, pp. 735–741, Oct 2014.

[18] R. Zhou, X. Li, T. C. Yang, Z. Liu, and Z. Wu, "Real-time cyclostationary analysis for cognitive radio via software defined radio," in *Proc. of IEEE Global Communications Conference (GLOBECOM)*, Anaheim, CA, Dec 2012.

[19] J. J. Popoola and R. V. Olst, "The performance evaluation of a spectrum sensing implementation using an automatic modulation classification detection method with a Universal Software Radio Peripheral," *Expert Systems with Applications*, vol. 40, no. 6, pp. 2165 – 2173, 2013.